



Reservoir Computing in R: a Tutorial for Using reservoirnet to Predict Complex Time-Series

ISSN 2824-7795

- Thomas Ferté Inserm Bordeaux Population Health Research Center UMR 1219, Inria BSO, team SISTM, F-33000 Bordeaux, France, Inserm
Inserm Bordeaux Population Health Research Center UMR 1219, Inria BSO, team SISTM, F-33000 Bordeaux, France, Inria
Bordeaux Hospital University Center, Pôle de santé publique, Service d'information médicale, F-33000 Bordeaux, France, CHU de Bordeaux
- Kalidou Ba Inserm Bordeaux Population Health Research Center UMR 1219, Inria BSO, team SISTM, F-33000 Bordeaux, France, Inserm
Inserm Bordeaux Population Health Research Center UMR 1219, Inria BSO, team SISTM, F-33000 Bordeaux, France, Inria
Bordeaux Hospital University Center, Pôle de santé publique, Service d'information médicale, F-33000 Bordeaux, France, CHU de Bordeaux
- Dan Dutartre Inria BSO, Inria
Pierrick Legrand Inria BSO, F-33000 Bordeaux, France, Inria
IMB, Institut de Mathématiques de Bordeaux, UMR CNRS 5251, IMB
- Vianney Jouhet Inserm Bordeaux Population Health Research Center UMR 1219, team AHeAD, F-33000 Bordeaux, Inserm
Bordeaux Hospital University Center, Pôle de santé publique, Service d'information médicale, F-33000 Bordeaux, France, CHU de Bordeaux
- Romain Griffier Inserm Bordeaux Population Health Research Center UMR 1219, team AHeAD, F-33000 Bordeaux, Inserm
Bordeaux Hospital University Center, Pôle de santé publique, Service d'information médicale, F-33000 Bordeaux, France, CHU de Bordeaux
- Rodolphe Thiébaut Inserm Bordeaux Population Health Research Center UMR 1219, Inria BSO, team SISTM, F-33000 Bordeaux, France, Inserm
Inserm Bordeaux Population Health Research Center UMR 1219, Inria BSO, team SISTM, F-33000 Bordeaux, France, Inria
Bordeaux Hospital University Center, Pôle de santé publique, Service d'information médicale, F-33000 Bordeaux, France, CHU de Bordeaux
- Xavier Hinaut Inria BSO, F-33000 Bordeaux, France, Inria
Univ. Bordeaux, CNRS, IMN, UMR 5293, Bordeaux, France, CNRS
LabRI, Univ. Bordeaux, Bordeaux INP, CNRS UMR 5800., LaBRI
- Boris Hejblum ¹Inserm Bordeaux Population Health Research Center UMR 1219, Inria BSO, team SISTM, F-33000 Bordeaux, France, Inserm
Inserm Bordeaux Population Health Research Center UMR 1219, Inria BSO, team SISTM, F-33000 Bordeaux, France, Inria

Date published: 2024-12-06 Last modified: 2024-12-06

Abstract

¹Corresponding author:

Reservoir Computing (RC) is a machine learning method based on neural networks that efficiently process information generated by dynamical systems. It has been successful in solving various tasks including time series forecasting, language processing or voice processing. RC is implemented in Python and Julia but not in R. This article introduces `reservoirnet`, an R package providing access to the Python API `ReservoirPy`, allowing R users to harness the power of reservoir computing. This article provides an introduction to the fundamentals of RC and showcases its real-world applicability through three distinct sections. First, we cover the foundational concepts of RC, setting the stage for understanding its capabilities. Next, we delve into the practical usage of `reservoirnet` through two illustrative examples. These examples demonstrate how it can be applied to real-world problems, specifically, regression of COVID-19 hospitalizations and classification of Japanese vowels. Finally, we present a comprehensive analysis of a real-world application of `reservoirnet`, where it was used to forecast COVID-19 hospitalizations at Bordeaux University Hospital using public data and electronic health records.

Keywords: Reservoir Computing, Covid-19, Electronic Health Records, Time series

1 Contents

2	1 Introduction	3
3	2 RC presentation	4
4	3 Usage workflow	6
5	3.1 Installation	6
6	3.2 Package workflow overview	6
7	3.3 Basic regression use-case	6
8	3.3.1 Covid-19 data	6
9	3.3.2 First reservoir	8
10	3.3.3 Forecast	9
11	3.4 Classification	11
12	3.4.1 The Japanese vowel dataset	11
13	3.4.2 Classification (sequence-to-vector model)	11
14	3.4.3 Transduction (sequence-to-sequence model)	13

15	4 Avanced case-study: Covid-19 hospitalizations forecast	14
16	4.1 Introduction	14
17	4.2 Methods	16
18	4.2.1 Data	16
19	4.2.2 Evaluation framework	16
20	4.2.3 Models	17
21	4.2.4 Hyperparameter optimisation using random search	17
22	4.3 Results	18
23	4.3.1 Hyperparameter selection	18
24	4.3.2 Forecast performance	22
25	4.3.3 Number of model to aggregate	22
26	4.3.4 Input feature importance	22
27	4.4 Discussion	26
28	5 Discussion and conclusion	26
29	References	28

30 **1 Introduction**

31 Reservoir Computing (RC) is a prominent machine learning method, proposed by Jaeger (2001),
 32 Maass, Natschläger, and Markram (2002) and Lukoševičius and Jaeger (2009) that has gained signifi-
 33 cant attention in recent years for its ability to efficiently process information generated by dynamical
 34 systems. This innovative approach leverages the dynamics of a high-dimensional “reservoir” (we
 35 define it below) to perform complex computations and solve various tasks based on the response of
 36 this dynamical system to input signals. RC has demonstrated its efficacy in tackling various chal-
 37 lenges, encompassing pattern classification and time series forecasting in applications ranging from
 38 electrocardiogram analysis to bird calls Trouvain and Hinaut (2021), language processing Hinaut
 39 and Dominey (2013), power plants, internet traffic, stock prices, and beyond Tanaka et al. (2019).

40 Originally, the RC paradigm was implemented in artificial firing-rate neurons (“Echo State
 41 Networks”, Jaeger (2001)) and spiking neurons (“Liquid State Machine”, Maass, Natschläger, and
 42 Markram (2002)) as a recurrent neural network (RNN) where the internal recurrent connections,
 43 denoted as the reservoir, are randomly generated and only the output layer (named “read-out”)
 44 is trained. The reservoir projects temporal input signals onto a high-dimensional feature space,
 45 facilitating the learning of non-linear and temporal interactions. Thus, this recurrent layer contains
 46 high-dimensional non-linear recombination of the inputs and past states: it is a “reservoir of
 47 computations” from which useful information can be linearly extracted (or “read-out”) to provide
 48 the desired outputs. This offers the advantage of decreasing the computing time compared to
 49 conventional RNNs while consistently maintaining performance (Vlachas et al. 2020). Besides,
 50 this RC paradigm fostered increasing interest thanks to its ability to be implemented on classical
 51 computers, as the hidden recurrent layer can be kept untrained. A wide range of physical media
 52 can be also used to replace it and Tanaka et al. (2019) recently reviewed this prolific field: from
 53 FPGA hardware (Penkovsky, Larger, and Brunner 2018), to spin waves using magnetic properties

54 (Nakane, Tanaka, and Hirose 2018), skyrmions (Prychynenko et al. 2018) or optical implementations
55 (Rafayelyan et al. 2020). This provides interesting and potentially more efficient alternative to
56 traditional machine learning computing.

57 RC leverages various hyperparameters to introduce prior knowledge about the relationship between
58 input variables and output targets. But because the connections within the reservoir are randomly
59 initialized, the same set of hyperparameters may exhibit diverse behaviors across different instances
60 of the reservoir connections. This unpredictability makes it challenging to anticipate the perfor-
61 mance of a particular hyperparameter setting, as identical settings may produce varying outcomes
62 when applied to distinct instances of the reservoir. Moreover, selecting the most suitable hyperpa-
63 rameters often requires researchers to experiment with multiple combinations on a training dataset
64 and evaluate their performance on a separate test set². Although this approach can be resource-
65 intensive and time-consuming, it is a compromise that is acceptable considering the rapid simu-
66 lation capabilities offered by RC. Furthermore, there is a current absence of implementation in R,
67 rendering the method challenging for users unfamiliar with Python (Trouvain and Hinaut 2022) or
68 Julia (Martinuzzi et al. 2022).

69 Here, we offer comprehensive guidance to assist new users in maximizing the benefits of RC. Ini-
70 tially, a broad introduction to reservoir computing is presented in Section 2, followed in Section 3
71 by a tutorial on its application using reservoirnet, an R package built upon the ReservoirPy Python
72 module Trouvain et al. (2020). Section 3 then introduces the workflow usage on reservoirnet for
73 RC with two basic use-cases, and finally, in Section 4 we investigate the various challenges associ-
74 ated with an advanced case-study leveraging RC for forecasting COVID-19 hospitalizations. This
75 case-study exploration includes detailed guidance on the modeling strategy, the selection of hyper-
76 parameters, and the implementation process.

77 2 RC presentation

78 RC is a machine learning paradigm which is most often implemented as Echo State Networks (ESNs),
79 i.e. the firing-rate neuron version (Jaeger 2001). An ESN is described by three matrices of connec-
80 tivity: an input layer W_{in} , a recurrent layer W and an output layer W_{out} . At each time step, the input
81 vector u_t is projected into the reservoir which is also combined with reservoir past state $x(t - 1)$
82 through the recurrent connections. The output $y(t)$ is linearly read-out from the reservoir. Input
83 W_{in} and recurrent W matrices are kept random; only the output matrix W_{out} is trained in an offline
84 or online method. Often a ridge regression (i.e.~a regularized linear regression) is used to obtain the
85 desired outputs $y(t)$ from the reservoir states $x(t)$. Figure 1 depicts the architecture. For simplicity,
86 we will use the term “reservoir computing” for “Echo State Network” in the remainder of the paper.

87 The input layer $u(t)$ is an M -dimension vector, where M is the number of input time series, which
88 corresponds to the values of the input time series at time t where $t = 1, \dots, T$. The reservoir layer
89 $x(t)$ is an N_{res} -dimensional vector where N_{res} is the number of nodes in the reservoir. The value $x(t)$
90 is defined as follow:

$$x(t + 1) = (1 - \alpha)x(t) + \alpha \tanh(Wx(t) + W_{in}u(t + 1)) \quad (1)$$

91 The leaking rate $\alpha \in [0, 1]$ defines the update rate of the nodes. The closer α is to 1, the more the
92 reservoir is sensitive to new inputs $u(t)$. Therefore, the reservoir state at time $t + 1$ denoted $x(t + 1)$
93 depends on the reservoir state at the previous time $x(t)$ and the new inputs $u(t + 1)$. Both W_{in} and
94 W are random matrices of size $N_{res} \times M$ and $N_{res} \times N_{res}$ respectively.

²In this article, we employ the term “train set” to refer to the combined dataset consisting of both the training and validation sets, which are cycled through in a cross-validation manner.

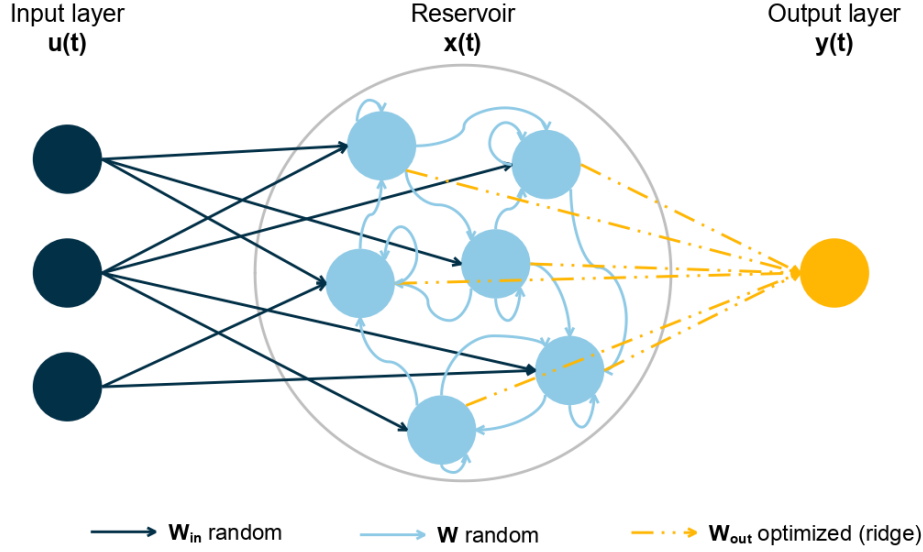


Figure 1: Reservoir computing is composed of an input layer, a reservoir and an output layer. Connection between input layer and reservoir and inside reservoir are random. Only the output layer is optimized based on a ridge regression. Adapted from Trouvain et al. (2020)

95 W_{in} is a matrix (usually sparse) generated using a Bernoulli (bimodal) distribution where each value
96 can be either $-I_{scale}(m)$ or $I_{scale}(m)$ with an equal probability where $m = 1, \dots, M$ corresponds to a
97 given feature in the input layer. The input scaling, denoted I_{scale} , is a hyperparameter coefficient
98 common to all features from the input layer or specific to each feature m . In that case, the more
99 important the feature is, the greater should be its input scaling. W is a matrix (usually sparse) where
100 values are generated from a Gaussian distribution $\mathcal{N}(0, 1)$. Then, the W matrix is scaled according
101 to the defined spectral radius, a hyperparameter defining the highest eigen value of W .

102 The final layer is a linear regression with ridge penalization where the explanatory features are the
103 reservoir state and the variable to be explained is the outcome to predict such that:

$$W_{out} = YX^T(XX^T + \lambda I)^{-1}$$

104 Where $x(t)$ and $y(t)$ are accumulated in X and Y respectively such that:

$$X = \begin{bmatrix} x(1) \\ x(2) \\ \vdots \\ x(T) \end{bmatrix} \text{ and } Y = \begin{bmatrix} y(1) \\ y(2) \\ \vdots \\ y(T) \end{bmatrix}$$

105 The parameter λ is the ridge penalization which aims to prevent overfitting. Additionally, one can
106 also connect the input layer to the output layer to the reservoir nodes. In that case, X is the accu-
107 mulation of both such that :

$$X = \begin{bmatrix} x(1), u(1) \\ x(2), u(2) \\ \vdots \\ x(T), u(T) \end{bmatrix} \text{ and } Y = \begin{bmatrix} y(1) \\ y(2) \\ \vdots \\ y(T) \end{bmatrix}$$

108 Overall, there are four main hyperparameters to be chosen by the user: i) the leaking rate which
109 defines the memory of the RC, ii) the input scaling which defines the relative importance of the
110 features, iii) the spectral radius which defines the connections of the neurons inside the reservoir
111 which in turn defines the degree of non-linear combination of features, and iv) the ridge penalization
112 which controls the degree of overfitting. The choice of hyperparameters often requires the user to
113 evaluate the performance of different combinations of hyperparameters on a validation set before
114 selecting the optimal combination to forecast on the test set.

115 **3 Usage workflow**

116 In this section, we will cover the basics of `reservoirnet` use including installation, classification
117 and regression. A more in depth description is provided in Section 4 with the covid-19 forecast use
118 case.

119 **3.1 Installation**

120 `reservoirnet` is an R package making the Python module `ReservoirPy` easily callable from R using
121 `reticulate` R package Ushey, Allaire, and Tang (2024). It is available on CRAN (see <https://cran.r-project.org/package=reservoirnet>) and can be installed using:

123 Reservoir Computing (RC) is well suited to both regression and classification tasks. We will intro-
124 duce a simple example for both task.

125 **3.2 Package workflow overview**

126 The workflow of `reservoirnet` is described in Figure 2. A reservoir model is created by the associa-
127 tion of an input layer (a matrix), a reservoir, and an output layer. Both the reservoir and the output
128 layer are created using the function `reservoirnet::createNode()` by specifying the node type (i.e.,
129 either `Reservoir` or `Ridge`).

130 This function accepts several arguments to specify the hyperparameters of the reservoir and will be
131 detailed in future sections. After the reservoir and output layer are created, they can be connected
132 using the `%>>%` operator, a specific pipe operator dedicated to `reservoirnet`. The model can then be
133 fitted using `reservoirR_fit()` and used to make predictions on a new dataset using `predict_seq()`.

134 **3.3 Basic regression use-case**

135 **3.3.1 Covid-19 data**

136 In this first use-case, we will introduce the fundamental usage of the `reservoirnet` package. This
137 demonstration will be conducted using the COVID-19 dataset that is included within the package.
138 These data encompass hospitalization, positive RT-PCR (Reverse Transcription Polymerase Chain
139 Reaction) results, and overall RT-PCR data sourced from Santé Publique France, which are publicly
140 available on data.gouv.fr (for further details, refer to `help(dfCovid)`). Our primary objective is to
141 predict the number of hospitalized patients 14 days into the future. To accomplish this, we will
142 initially train our model on data preceding the date of January 1, 2022, and subsequently apply it to
143 forecast values using the subsequent dataset.

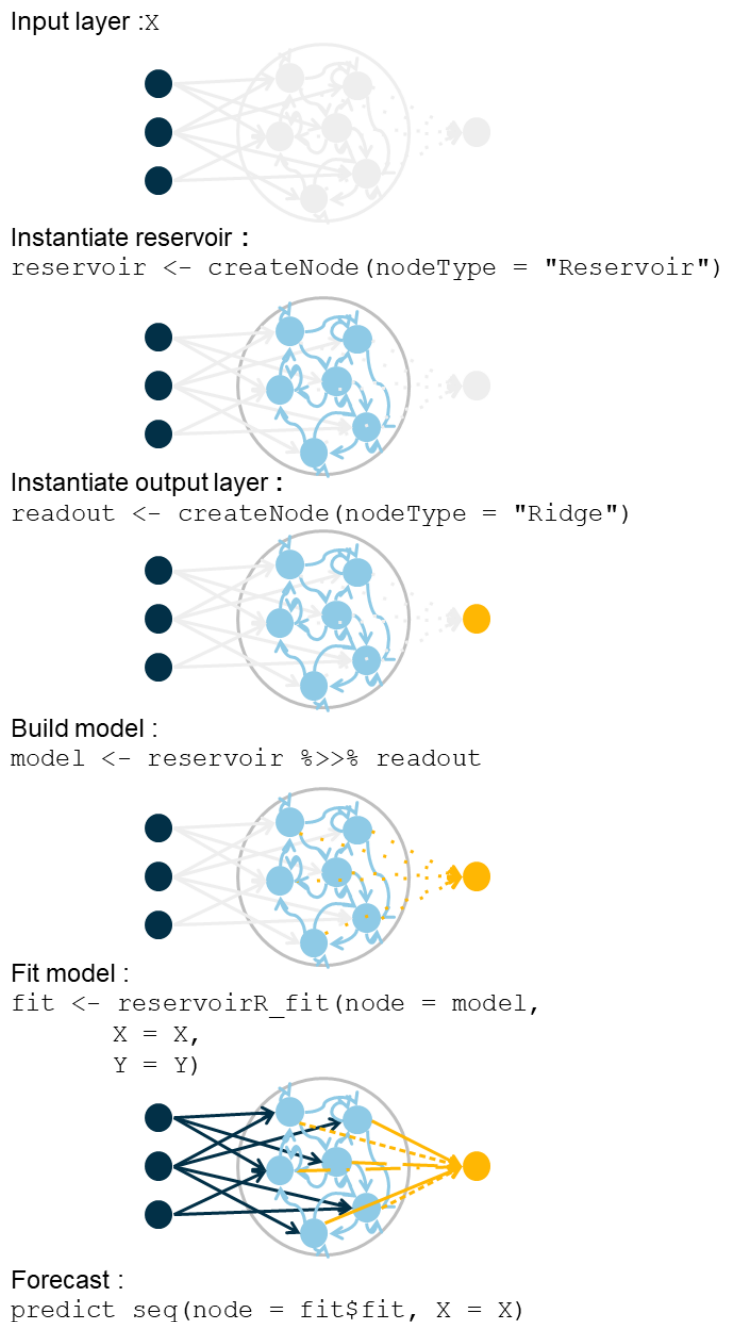


Figure 2: Workflow of `reservoirnet`.

144 We can proceed by loading useful packages - namely `ggplot2` Wickham, Navarro, and Pedersen
145 (2018) and `dplyr` Wickham et al. (2023), data and define the task:

146 Due to the substantial fluctuations observed in both RT-PCR metrics, our initial step involves ap-
147 plying a moving average computation over the most recent 7-day periods for these features. Addi-
148 tionally, we augment the dataset by introducing an `outcome` column and an `outcomeDate` column,
149 which will serve as valuable inputs for model training. Moreover, we calculate the `outcome_deriv`
150 as the difference between the `outcome` and the number of hospitalized patients (`hosp`), represent-
151 ing the variation in hospitalization in relation to the current count of hospitalized individuals. The
152 resulting smoothed data is visualized in Figure 3.

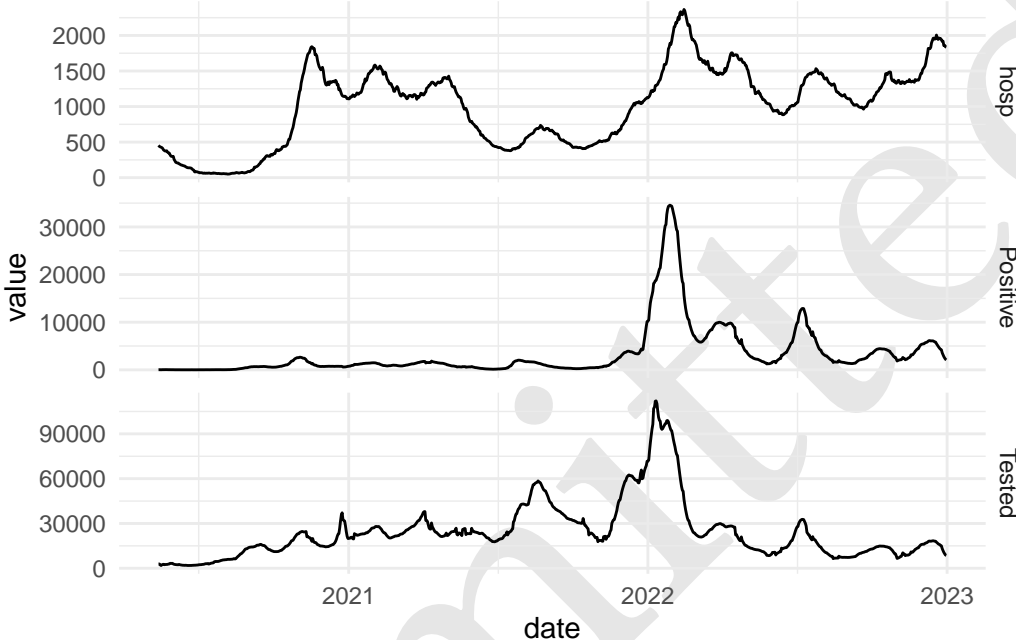


Figure 3: Hospitalizations, IPTCC and positive PCR of Bordeaux University Hospital.

153 3.3.2 First reservoir

154 Setting a reservoir is done with the `createNode()` function. The important hyperparameters are the
155 following :

- 156 • Number of nodes (`units`) : it corresponds to the number of nodes inside the reservoir. Usually,
157 the more the better, but more nodes increases the computation time.
- 158 • Leaking rate (`lr`) : the leaking rate corresponds to the balance between the new inputs and
159 the previous state. A leaking rate of 1 only consider information from new inputs.
- 160 • Spectral radius (`sr`): the spectral radius is the maximum absolute eigenvalue of the reservoir
161 connectivity matrix. A small spectral radius induces stable dynamics inside the reservoir, a
162 high spectral radius induces a chaotic regime inside the reservoir.
- 163 • Input scaling (`input_scaling`): the input scaling is a gain applied to the input features of the
164 reservoir.
- 165 • Warmup (`warmup`) : it corresponds to the number of time step during which the data are
166 propagating into the reservoir but not used to fit the output layer. This hyperparameter is set
167 in the `reservoirR_fit()` function.

168 In addition, we can set the seed (`seed`). Because the reservoir connections are set at random, setting
169 the seed is a good approach to ensure reproducibility.

170 For this part of the tutorial, we will set the hyperparameter at a given value. Hyperparameter
171 optimization will be detailed at Section 4.

172 Then we can feed the data to the reservoir and see the activation state of the reservoir $x(t)$. To do
173 so, we first prepare the data and transform it to a matrix:

174 Then we run the `predict_seq()` function. It takes as input a node (i.e a reservoir or a reservoir
175 associated with an output layer) and the feature matrix.

176 Now we can visualize node activation using the `plot()` function presented at Figure 4 .

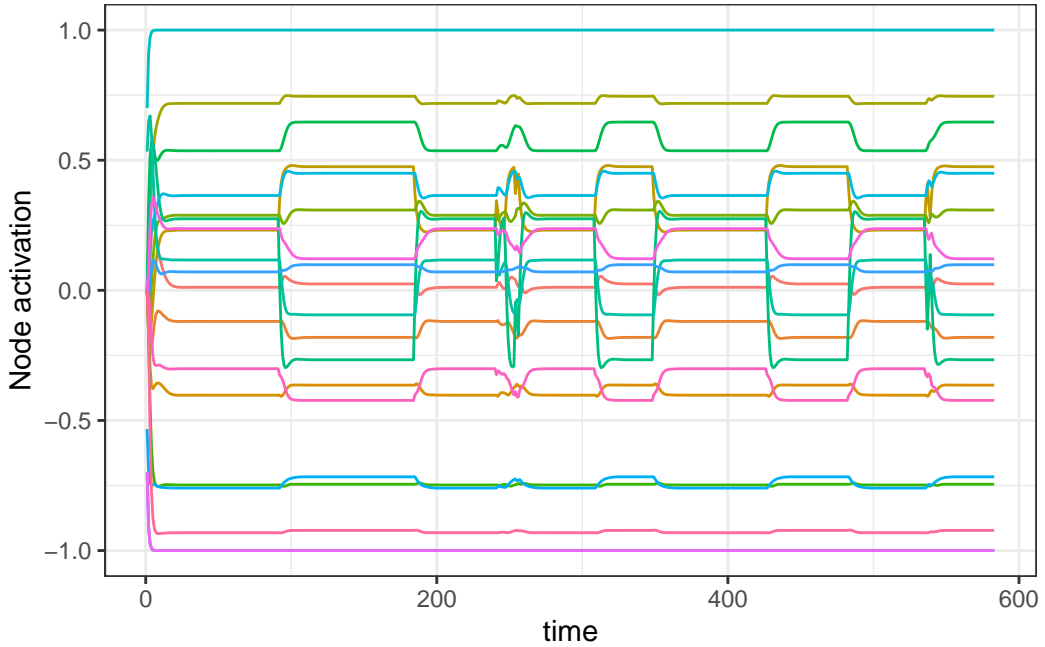


Figure 4: 20 random nodes activation over time.

177 Numerous nodes within the system exhibit a consistent equilibrium state. The challenge arises when
178 the output layer attempts to extract knowledge from these nodes, as they do not convey meaningful
179 information. This issue can be attributed to the disparate scales of the features. To address this
180 concern, a practical approach involves normalizing the features by dividing each of them by their
181 respective maximum values, thereby scaling them within the range of -1 to 1 by dividing by the
182 maximum of the absolute value. Of note, here the features will be scaled between 0 and 1 because
183 all features are positive.

184 We then feed them to the reservoir and plot the node activation again. Compared to Figure 4, the
185 obtained node activation at Figure 5 shows interesting trend outputs as no node seems saturated.

186 3.3.3 Forecast

187 In order to train the reservoir, we should train the last layer which linearly combines the neuron's
188 output.

189 3.3.3.1 Set the ESN

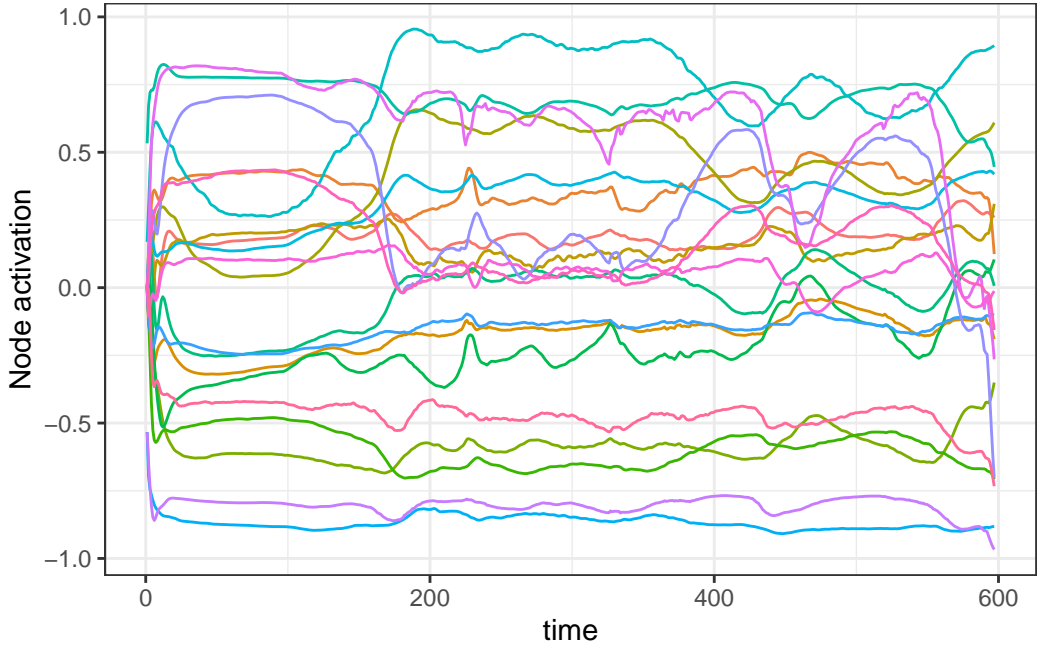


Figure 5: 20 random node activation over time. Scaled features.

Initially, we establish the output layer, incorporating a ridge penalty set at $1e3$. It's important to note that this hyperparameter can be subject to optimization, a topic that will be explored in Section 4. This parameter plays a pivotal role in fine-tuning the model's conformity to the data. When set excessively high, the risk of underfitting arises, whereas setting it too low can lead to overfitting. We connect the output layer to the reservoir making the model ready to be trained.

3.3.3.2 Set the data

First we separate the train set on which we will learn the ridge coefficients and the test set on which we will make the forecast. We define the train set to be all the data before 2022-01-01 and the test data to be all the data to have forecast both on train and test sets.

We standardize with the same formula as seen before. We learn the standardization on the training set and apply it on the test set. Then we convert the dataframe to matrix.

3.3.3.3 Train the model and predict

We then feed the reservoir with the train set. To do so, we set a warmup of 30 days during which the data are propagating into the reservoir but not used to fit the output layer.

Fitting node Ridge-0...

Now that the ridge layer is trained, we can forecast. We set the parameter `reset` to `TRUE` in order to clean the reservoir from the data used by the training set.

We observe that the model forecast at Figure 6 is not fully accurate, both on the test set and the train set. In that case, one option could be to reduce ridge penalization to fit more closely the data, the optimization of ridge hyperparameter will be discussed at Section 4. Another possibility is to ease the learning of the algorithm by forecasting the variation of the hospitalization instead of

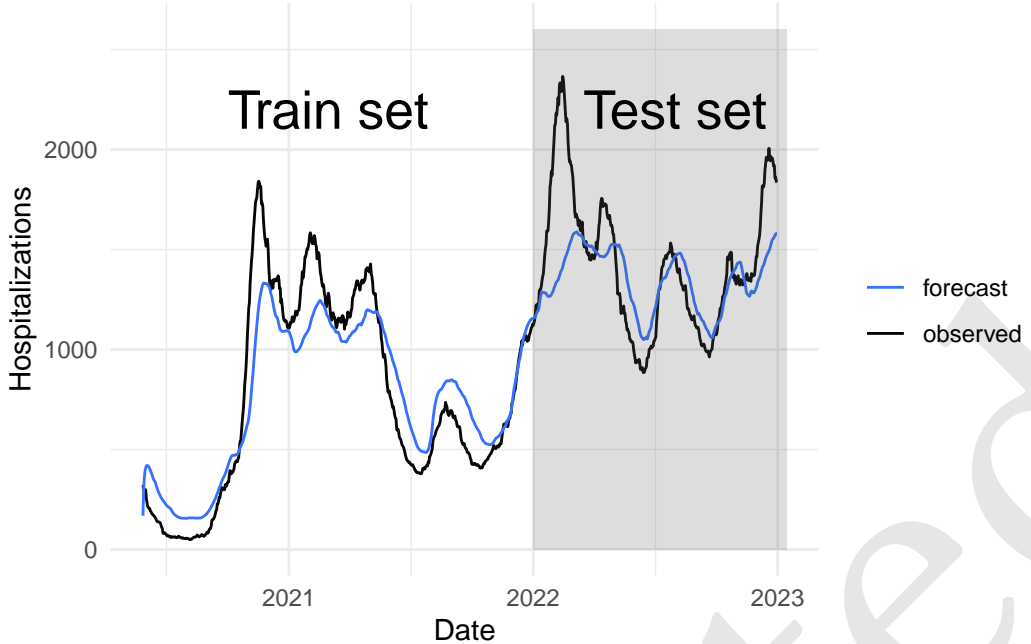


Figure 6: Forecast

211 the number of hospitalized patients. For that step, we will learn on the `outcome_deriv` contained
 212 in `yTrain_variation` data which is defined outcome as `outcome_deriv = outcome - hosp.`. As
 213 depicted at Figure 7, this strategy improved the model forecast.

214 Fitting node Ridge-0...

215 **3.4 Classification**

216 **3.4.1 The Japanese vowel dataset**

217 This example is largely inspired from the [classification tutorial of reservoirpy](#). To illustrate the
 218 classification task, we will use the Japanese vowel dataset (Kudo, Toyama, and Shimbo (1999)). The
 219 data can be loaded from `reservoirnet` as follow :

220 The dataset comprises 640 vocalizations of the Japanese vowel æ, contributed by nine distinct speak-
 221 ers. Each vocalization represents a time series spanning between 7 and 29 time steps, encoded as
 222 a 12-dimensional vector denoting the Linear Prediction Coefficients (LPC). A visual representation
 223 of six distinct utterances from the test set, originating from three different speakers, is depicted in
 224 Figure 8.

225 The primary objective involves the attribution of each utterance to its respective speaker, this is
 226 denoted as classification or sequence-to-vector encoding. The secondary objective involves the
 227 attribution of each time step of each utterance to its speaker, this is denoted as transduction or
 228 sequence-to-sequence encoding.

229 **3.4.2 Classification (sequence-to-vector model)**

230 The first approach is the sequence-to-vector encoding. For this task we aim to predict the speaker
 231 of the whole utterance (i.e the label is assigned to the whole sequence). We first start by creating

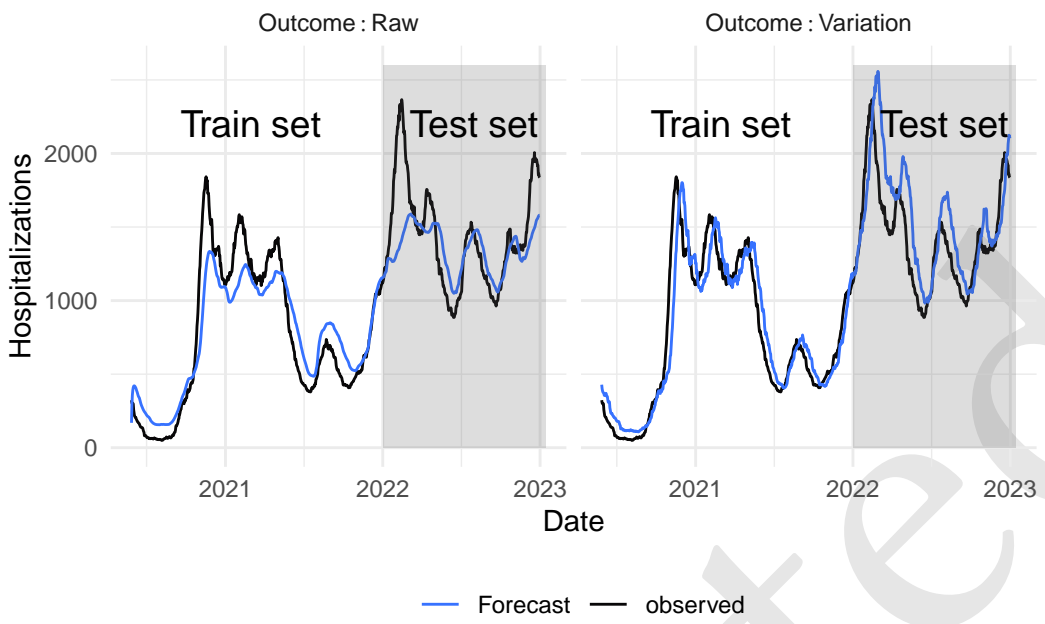


Figure 7: Covid-19 hospitalizations forecast. The model is either trained to forecast the number of hospitalizations (denoted Raw) or the variation of the hospitalizations compared to current level of hospitalisation (denoted Variation)



Figure 8: Vowel dataset, sample with 3 speakers and 2 utterance each.

232 the reservoir and the output layer.

233 To perform this task, we need to modify the training and testing processes. Leveraging the inherent
234 inertia of the reservoir, information from preceding time steps is preserved, effectively endowing
235 the RC with a form of memory. Consequently, the final state vector encapsulates insights gathered
236 from all antecedent states. In the context of the sequence-to-vector encoding task, only this ultimate
237 state is employed. This process is executed as follows:

238 Then we can train the readout based on this last state vector. In that case, Y_train contains a single
239 label for each utterance.

240 The prediction is also modified using only the final state :

241 Figure 9 shows the prediction for the 6 utterances depicted at Figure 8 where the model correctly
242 identifies the speaker.

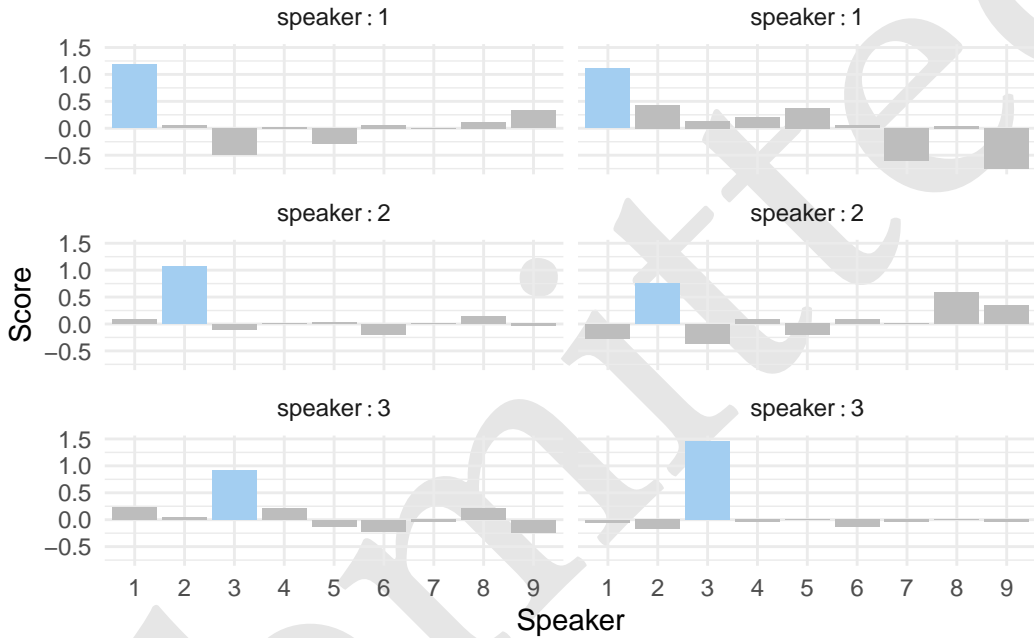


Figure 9: Prediction in a sequence-to-sequence approach 6 samples with 3 speakers and 2 utterance each. The speaker to predict is depicted in blue. For each of the 6 utterance, the model correctly identifies the speaker.

243 Then, we can also compute the overall accuracy :

244 [1] "Accuracy: 92.703%"

245 3.4.3 Transduction (sequence-to-sequence model)

246 For this task, the goal is to predict the speaker for each time step of each utterance. The first
247 step is to get the data where the label is repeated for each time step. This is easily done with the
248 repeat_targets argument as follow :

249 Then we can train a simple Echo State Network to solve this task. For this example we will connect
250 both the input layer and the reservoir layer to the readout layer which is performed by the %>>%
251 operator :

252 We can then fit the model and predict the labels for the test data. The `reset` parameter is set to TRUE
253 to remove information from the reservoir from the training process.

254 Fitting node Ridge-2...

255 From the `Y_pred` and `Y_test` we represent at Figure 10 the predictions for the same patients as in
256 Figure 8.

257 For those 6 utterances, the model correctly identify the speaker for most of the time steps. We can
258 then evaluate the overall accuracy of the model :

259 [1] "Accuracy: 92.456%"

260 4 Avanced case-study: Covid-19 hospitalizations forecast

261 4.1 Introduction

262 Since late 2020, millions of cases of SARS-CoV-2 infection have been documented across the globe
263 Carrat et al. (2021). This ongoing pandemic has exerted significant strain on healthcare systems,
264 resulting in a surge in hospitalizations. This surge, in turn, necessitated modifications to the health-
265 care infrastructure and gave rise to population-wide lockdown measures aimed at preventing the
266 saturation of healthcare facilities Kim et al. (2020). The capacity to predict the trajectory of the epi-
267 demic on a regional scale is of paramount importance for effective healthcare system management.

268 Numerous COVID-19 forecasting algorithms have been proposed using different methods (e.g en-
269 semble, deep learning, compartmental), yet none has proven entirely satisfactory Rahimi, Chen, and
270 Gandomi (2021). In France, short-term forecasts with different methods have been evaluated with
271 similar results Pottier (2021). In this context a machine learning algorithm based on linear regres-
272 sion with elastic-net penalization, leveraging both Electronic Health Records (EHRs) and public data,
273 was implemented at Bordeaux University Hospital (Ferté et al. 2022). This model, which aimed at
274 forecasting the number of hospitalized patients at 14 days, showed good performance but struggled
275 to accurately anticipate dynamic shifts of the epidemic.

276 RC has been used in the context of covid-19 epidemic forecast Ghosh et al. (2021). Among them,
277 Ghosh et al. (2021), Liu et al. (2023) and Ray, Chakraborty, and Ghosh (2021) used it to forecast
278 epidemic, Zhang et al. (2023) performed sentiment analysis and Kmet and Kmetova (2019) used
279 it to solve optimal control related to vaccine. The evaluation of RC for epidemic forecast showed
280 promising results in all approaches, being competitive with Long-Short Term Memory (LSTM) and
281 Feed-Forward Neural Network (FFNN) in Ray, Chakraborty, and Ghosh (2021). However, the test
282 period was short for Ghosh et al. (2021) (21 and 14 days) and Ray, Chakraborty, and Ghosh (2021)
283 (86 days) making it difficult to evaluate the behavior of the methods during epidemic dynamic shift.
284 This was not the case for Liu et al. (2023) (6 months) but they implemented daily ahead forecast
285 which would be difficult to use to manage a hospital. Finally, all three implementations used only
286 one time series as input whereas it has been shown that using different data sources could improve
287 forecast Ferté et al. (2022). Therefore, it is still difficult to assess the usefulness of RC over a large
288 period and using many time series as inputs.

289 RC can be viewed as an extension of penalized linear regression, where inputs undergo processing
290 by a reservoir, introducing the capacity for memory and non-linear combinations. Given the effec-
291 tiveness of penalized linear regression in COVID-19 forecasting, as highlighted in Ferté et al. (2022),

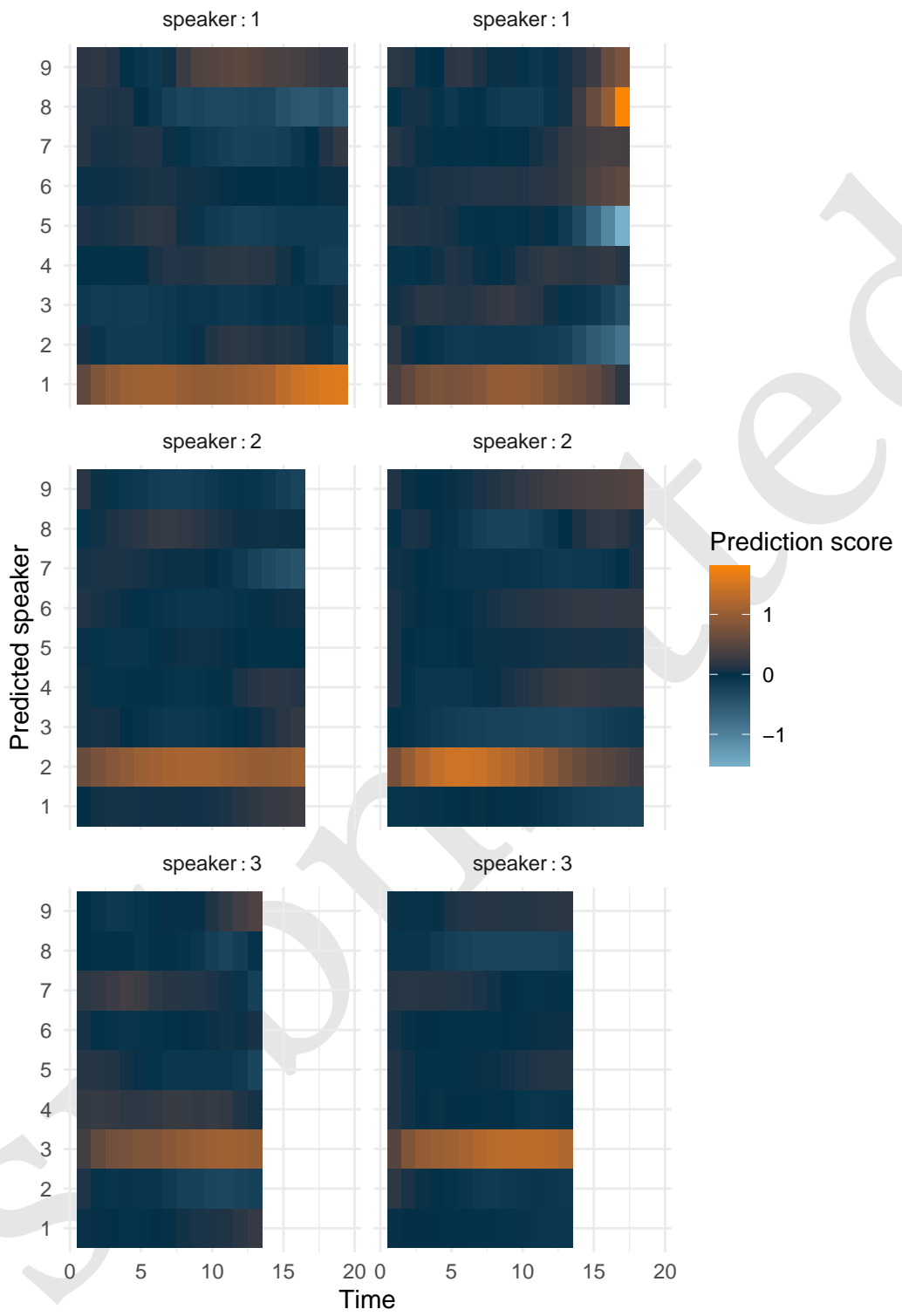


Figure 10: Prediction in a sequence-to-sequence approach 6 samples with 3 speakers and 2 utterance each. The higher the score of the speaker, the lighter the color.

and the promising results exhibited by RC in epidemic forecasting, as demonstrated in studies such as Ghosh et al. (2021), Liu et al. (2023), and Ray, Chakraborty, and Ghosh (2021), we have opted to employ RC for the prediction of hospitalizations at 14 days at the University Hospital of Bordeaux. The primary aim of this study is to assess the performance of RC in this forecasting task. Secondary objectives include (i) comparing the performance of RC with that of elastic-net penalized regression (identified as the optimal model in Ferté et al. (2022)) and (ii) evaluating variations in RC performance based on different architectural choices, such as the connection between the input layer and the output layer, and the use of one input scaling per feature versus a common input scaling.

4.2 Methods

4.2.1 Data

The study utilized aggregated data spanning from May 16, 2020, to January 17, 2022, regarding the COVID-19 epidemic in France, drawing from various sources to enhance forecasting accuracy. These sources encompassed epidemiological statistics from Santé Publique France, weather data from the National Oceanic and Atmospheric Administration (NOAA), both providing department-level data Etalab (2020) and Electronic Health Record (EHR) data from the Bordeaux Hospital providing hospital-level data. All data were daily updated. Santé Publique France data included information on hospitalizations, RT-PCR tests, positive RT-PCR results, variant prevalence, and vaccination data, categorized by age groups. NOAA data contributed temperature, wind speed, humidity, and dew point data, allowing for the computation of the COVID-19 Climate Transmissibility Predict Index (Roumagnac et al. 2021). EHRs data included hospitalizations, ICU admissions, ambulance service records, and emergency unit notes, with relevant COVID-19-related concepts extracted from the notes. Data are discussed more in depth in Ferté et al. (2022).

First derivative over the last 7 days were computed to enrich model information. To take into account measurement error and daily noise variation, data were smoothed using a local polynomial regression with a span of 21 days. As previously described, input features were scaled between -1 and 1 by dividing the observed value by the maximum of the absolute value of the given input feature.

All data are publicly available. Weather data can be obtained from Smith, Lott, and Vose (2011) using R package `worldmet` (Carslaw 2023). Vaccine data can be downloaded from Etalab (2020). EHRs data can be downloaded on dryad (Ferté et al. 2023). For privacy issues, publicly available EHRs data below 10 patients were obfuscated to 0. For convenience, all data were downloaded, merged and provided as replication material.

4.2.2 Evaluation framework

The task was to forecast 14 days ahead the number of hospitalized patients. As seen at Section 3.3, we will train the model to predict the variation of hospitalization, denoted as $hosp$, defined as $outcome_{t+14} = hosp_{t+14} - hosp_t$. Metrics computation and visualizations will be performed on the predicted number of hospitalizations denoted as $\widehat{hosp}_{t+14} = \widehat{outcome}_{t+14} + hosp_t$.

The dataset was separated into two periods. First period from May 16, 2020 to March 1, 2021 served to identify relevant hyperparameters. Remaining data was used to evaluate the model performance.

The performance of the model was evaluated according to several metrics:

- the mean absolute error : $MAE = \text{mean}(|\widehat{hosp}_{t+14} - hosp_{t+14}|)$.

- the median relative error : $MRE = \text{median}(|\frac{\widehat{\text{hospt}_{t+14}} - \text{hospt}_{t+14}}{\text{hospt}_{t+14}}|)$.
- the mean absolute error to baseline : $MAEB = \text{mean}(|\widehat{\text{hospt}_{t+14}} - \text{hospt}_{t+14}| - |\text{hospt}_t - \text{hospt}_{t+14}|)$.
- the median relative error to baseline : $MREB = \text{median}(|\frac{\widehat{\text{hospt}_{t+14}} - \text{hospt}_{t+14}}{\text{hospt}_t - \text{hospt}_{t+14}}|)$

Median was chosen over mean for MRE and $MREB$ because those metrics tend to have extremely high values when the denominator is close to 0 (i.e when the number of hospitalized patients is close to 0 or the number of patients hospitalized at 14 days is close to the current number of hospitalized patients respectively). $MAEB$ and $MREB$ compare model performance to a baseline model which predicts the current number of hospitalized patients at 14 days. Those metrics help to determine the information added by the model and is a good baseline as covid-19 forecast model do not always outperform this basic forecast (Cramer et al. (2022)).

Because the outcome is obfuscated below 10 hospitalizations for privacy reason, we set both the outcome and the forecast to 10 when the observed value was 0 or the forecasted value was below 10 when evaluating the model performance.

4.2.3 Models

We compared RC to elastic-net penalized regression (denoted as Enet). Furthermore we evaluated RC based on several architectures. First we compared RC with a single input scaling common to all features and a RC with on specific input scaling per feature. Second we compared RC where the input layer is connected to the output layer in addition to the connection between reservoir and output layer. Therefore, five models were evaluated :

- Elastic-net penalized regression denoted *Enet*
- RC with a single input scaling and no connection between input and ouput layers denoted *Common IS R %»% O*
- RC with a single input scaling and connection between input and ouput layers denoted *Common IS I+R %»% O*
- RC with multiple input scaling and no connection between input and ouput layers denoted *Multiple IS R %»% O*
- RC with multiple input scaling and connection between input and ouput layers denoted *Multiple IS I+R %»% O*

Because of the randomness of the reservoir, we took the median forecast of 10 reservoir on the train set to evaluate the performance of a given hyperparameter set. On the test set we aggregated the forecast of 40 reservoirs, each of them having one of the 40 best hyperparameter sets found on the train set. In addition, because covid-19 hospitalization is a non-stationary process, models were re-trained everyday using all previous days. To ease computation burden, only one day over two was used to find hyperparameters on the training set.

4.2.4 Hyperparameter optimisation using random search

RC relies mainly on 4 hyperparameters including the leaking rate (i.e “memory” parameter), spectral radius (i.e “chaoticity” parameter), input scaling (i.e “feature gain” parameter) and ridge (i.e penalization parameter). Input scaling can be either, common to all features or specific to each feature which increases the number of hyperparameter by the number of features.

372 Following the notation from `glmnet` package (Friedman, Hastie, and Tibshirani 2010), elastic-net
373 penalized linear regression relies on two hyperparameters, `lambda` (i.e the penalization parameter)
374 and `alpha` (i.e the compromise between lasso and ridge penalty)

375 Hyperparameter were selected in the training set (i.e before March 1, 2021) using a wrapper approach
376 and a random search sampler using 2000 samples for each model. The sampling distribution were
377 defined as follow :

- 378 • (RC) ridge and (Enet) `lambda` : log-uniform law defined between 1e-10 and 1e5
379 • (RC) input scaling and spectral radius : log-uniform law defined between 1e-5 and 1e5
380 • (RC) leaking rate : log-uniform law defined between 1e-3 and 1
381 • (Enet) `alpha` : uniform defined between 0 and 1

382 We provided large search space for all hyper-parameters. Search space was slightly reduced for
383 leaking rate based on previous results and because a leaking rate of 1e-3 already imply that new
384 inputs make the reservoir change really slowly which is not inline with the dynamic of covid-19 but
385 would be appropriate for an application where the phenomena to forecast has a slow dynamic.

386 Finally, we provided an additional Enet model similar to the one in Ferté et al. (2022) where `alpha`
387 was set to 0.5 and `lambda` was re-evaluated everyday in the test set based on previous data using
388 the cross-validation procedure provided by `glmnet`.

389 **4.3 Results**

390 The goal of this task is to predict 14 days ahead the hospitalization. Figure Figure 11 shows both the
391 training set (i.e before 2021-03-01) and the test set where the blue curve correspond to the input fea-
392 tures (first derivatives are not shown) and the orange curves correspond to the outcome the model is
393 trained on (i.e the hospitalization variation) and the hospitalizations at 14 days on which the per-
394 formance metrics are computed. The figures outline that the relation between the input features and
395 the outcome evolve over time and that the time series is not stationary. For instance IPTCC (*Index*
396 *PREDICT de Transmissivité Climatique de la COVID-19*) seems correlated to the outcome except that
397 it completely miss the summer 2021 increase.

398 **4.3.1 Hyperparameter selection**

399 Figure Figure 12 shows the hyperparameter optimisation using random search for the different RC
400 architectures. We observe that model with multiple input scaling achieved better performance on
401 the train set compared to model with single input scaling which is expected as they can adapt more
402 closely to the data thanks to specific input scaling for each feature.

403 As expected, we observe that the optimal leaking rate is above 1e-2 for all RC which is coherent
404 with the short term dynamic of covid-19 epidemic. Trend for other hyperparameter are less clear
405 even though best hyperparameter sets were close for RC with common input scaling and for RC
406 with multiple input scaling.

407 Figure Figure 13 shows the hyperparameter search for RC with multiple input scaling and connected
408 input layer. We observe that the random search tend to favor high importance given to derivative
409 of positive RT-PCR (including the elderly) and the derivative of IPTCC. The rest of the feature do
410 not show clear pattern.

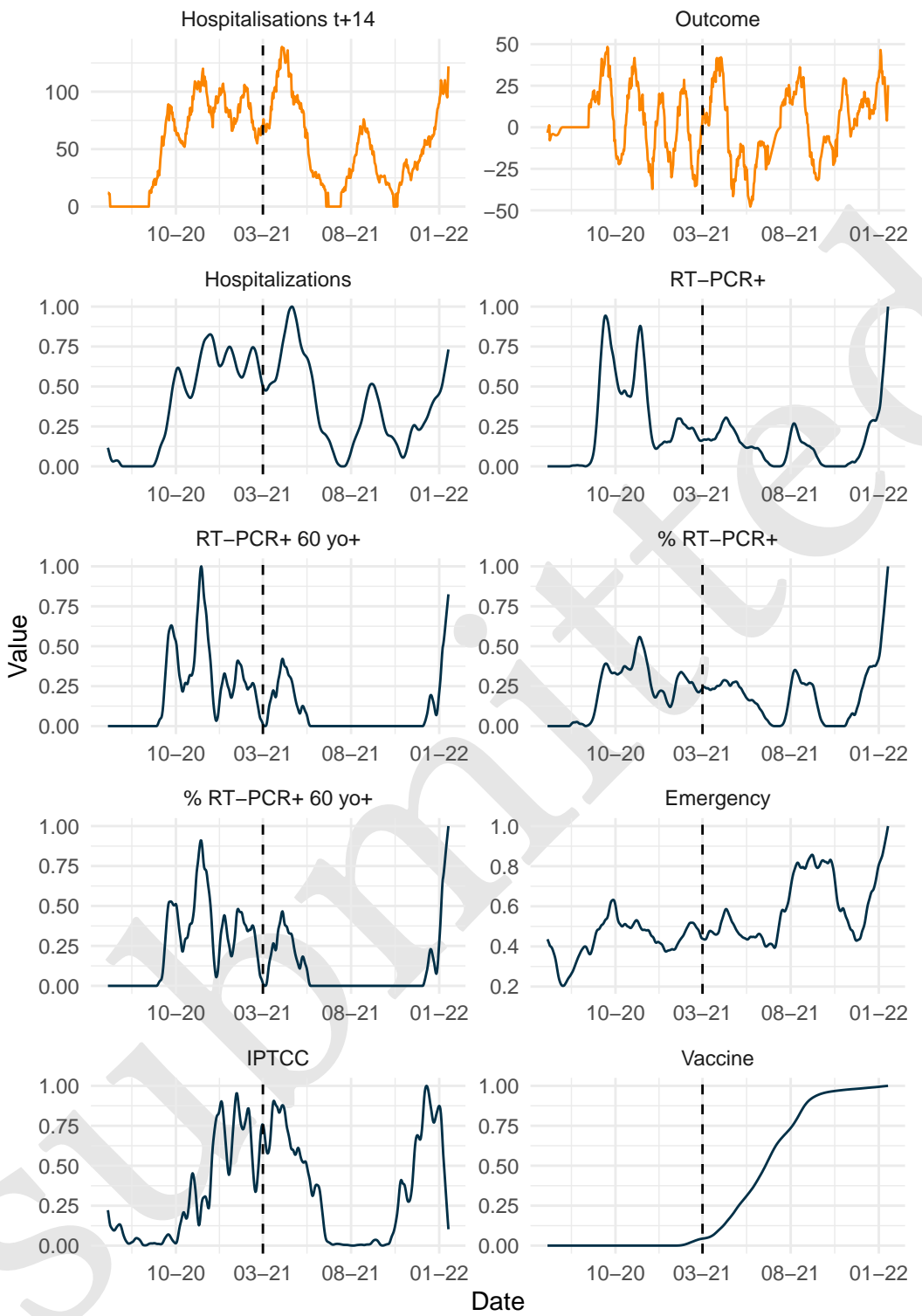


Figure 11: Covid-19 epidemic at BUH. Outcome of interest is presented in orange. Model is trained to forecast Outcome curve which corresponds to the difference between Hospitalisations at 14 days and current hospitalisations. Other features are scaled (divide by the maximum of the feature) represented in darkblue.

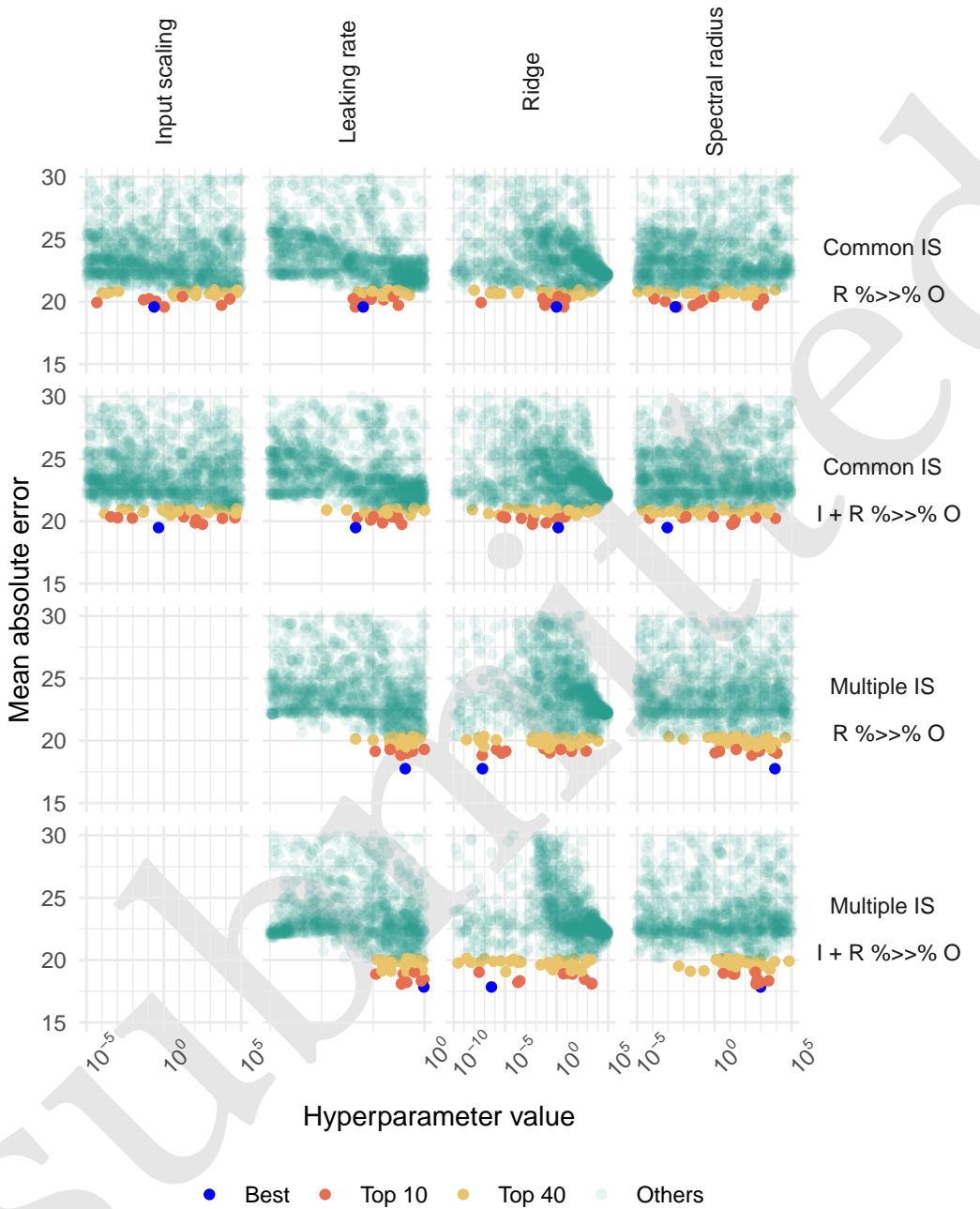


Figure 12: Hyperparameter evaluation on training set by random search. Hp sets with MAE above 30 were removed for clarity of visualisation.

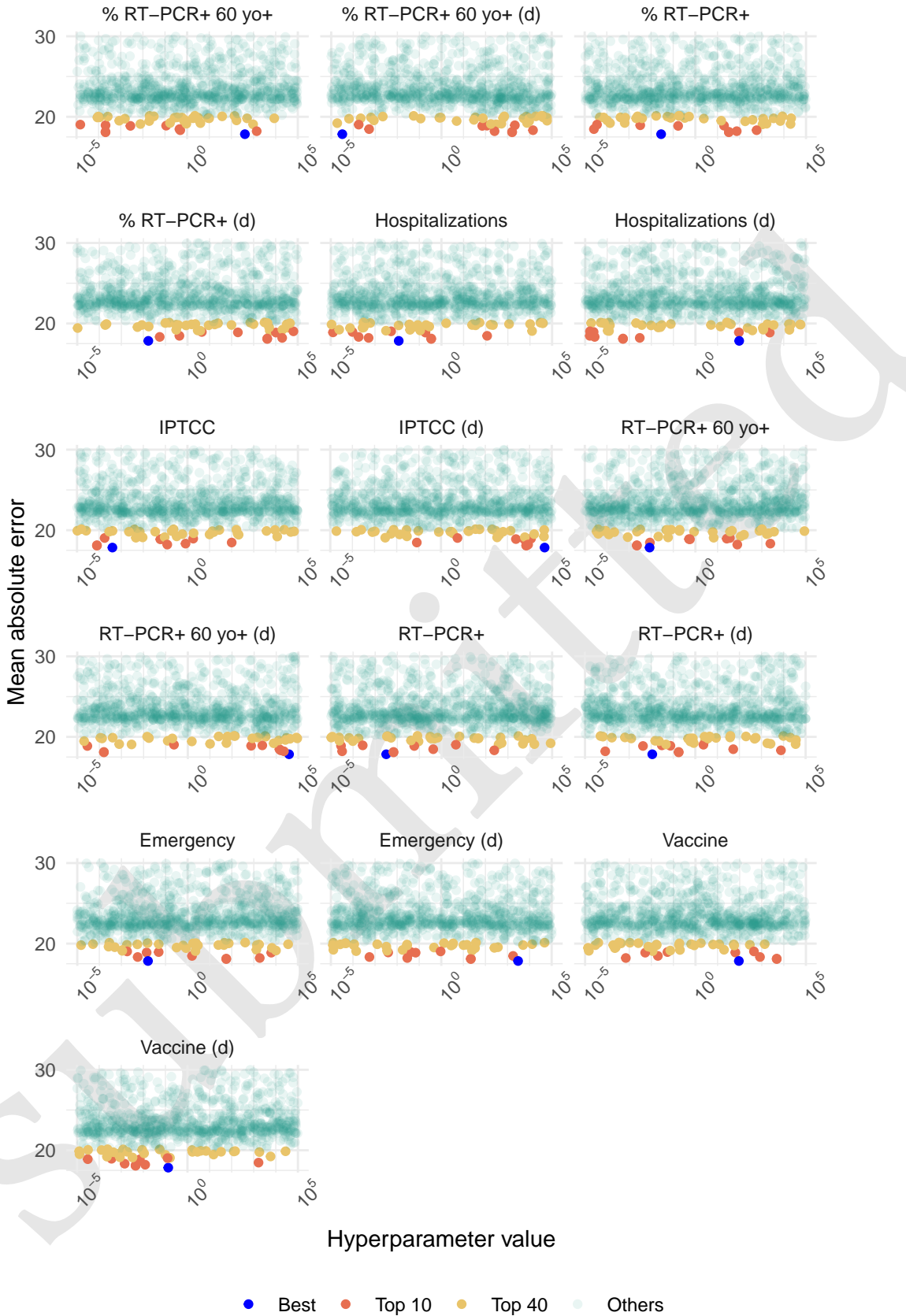


Figure 13: Hyperparameter evaluation on training set by random search of the model with multiple input scaling and no connection between input layer and output layer. Hp sets with MAE above 30 were removed for clarity of visualisation.

Table 1: Model performance with several reservoir configuration. For each setting, 40 reservoirs are computed and the forecast is the median of the 40 forecasts. Results show the performance metrics : MAE = Mean Absolute Error, MRE = Median Relative Error, MAEB = Mean Absolute Error to Baseline, MREB = Median Relative Error to Baseline.

Model Performance

Model	MAE	MRE	MAEB	MREB
Common IS R %»% O	15.23	0.26	-3.50	0.85
Common IS I + R %»% O	14.84	0.26	-3.89	0.83
Multiple IS R %»% O	15.38	0.28	-3.35	0.82
Multiple IS I + R %»% O	15.25	0.28	-3.49	0.83
Elastic-net	16.40	0.29	-2.34	0.93

411 4.3.2 Forecast performance

412 Table 1 shows the performance on the test set. Best model according to all metrics was RC with
413 common input scaling and connection between input and output layers. Having one input scaling
414 per feature did not improve the model which might be due to low generalisability of the hyperpa-
415 rameter of the training set to the test set due to non-stationarity. Additionally, connecting input layer
416 to output layer improved the model forecast. All RC models performed better than the elastic-net
417 model.

418 Figure 14 shows the forecast of the different models. We note that models struggle to accurately
419 forecast slope shifts. For instance, summer 2021 initial increase is partially predicted by all models
420 but its decrease is not well predicted. Winter 2021 increase is anticipated by all models but they
421 tend to overestimate it because of the rise of vaccine effect.

422 4.3.3 Number of model to aggregate

423 Figure 15 show the individual forecast for the 40 best sets of hyperparameters of each RC architec-
424 ture. Due to the internal random connection of the reservoir, we observe forecast stochasticity and
425 relying on only one forecast is unreliable. We explored the number of model needed at Figure 16
426 which shows that after 10 models, forecast is stable and even 5 models for the simpler model with
427 common input scaling which rely on less hyperparamters.

428 4.3.4 Input feature importance

429 We compared the coefficients of the output layer estimated for the input layer and the reservoir
430 nodes. Additionally, we compared the coefficient given to the input layer by the output layer in the
431 reservoir and the coefficient estimated by the elastic-net model.

432 Figure 17 illustrates the ranking of input layer compared to all connections to the output layer,
433 including the 500 reservoir nodes and the 16 features of the input layer (excluding bias). The figure
434 shows that the model with common input scaling tends to assign less weight to input layer compared
435 to the model with multiple input scaling. This suggests that the reservoir with common input scaling
436 provides more information than the reservoir with multiple input scaling, which aligns with its
437 better performance, as shown in Table Table 1.

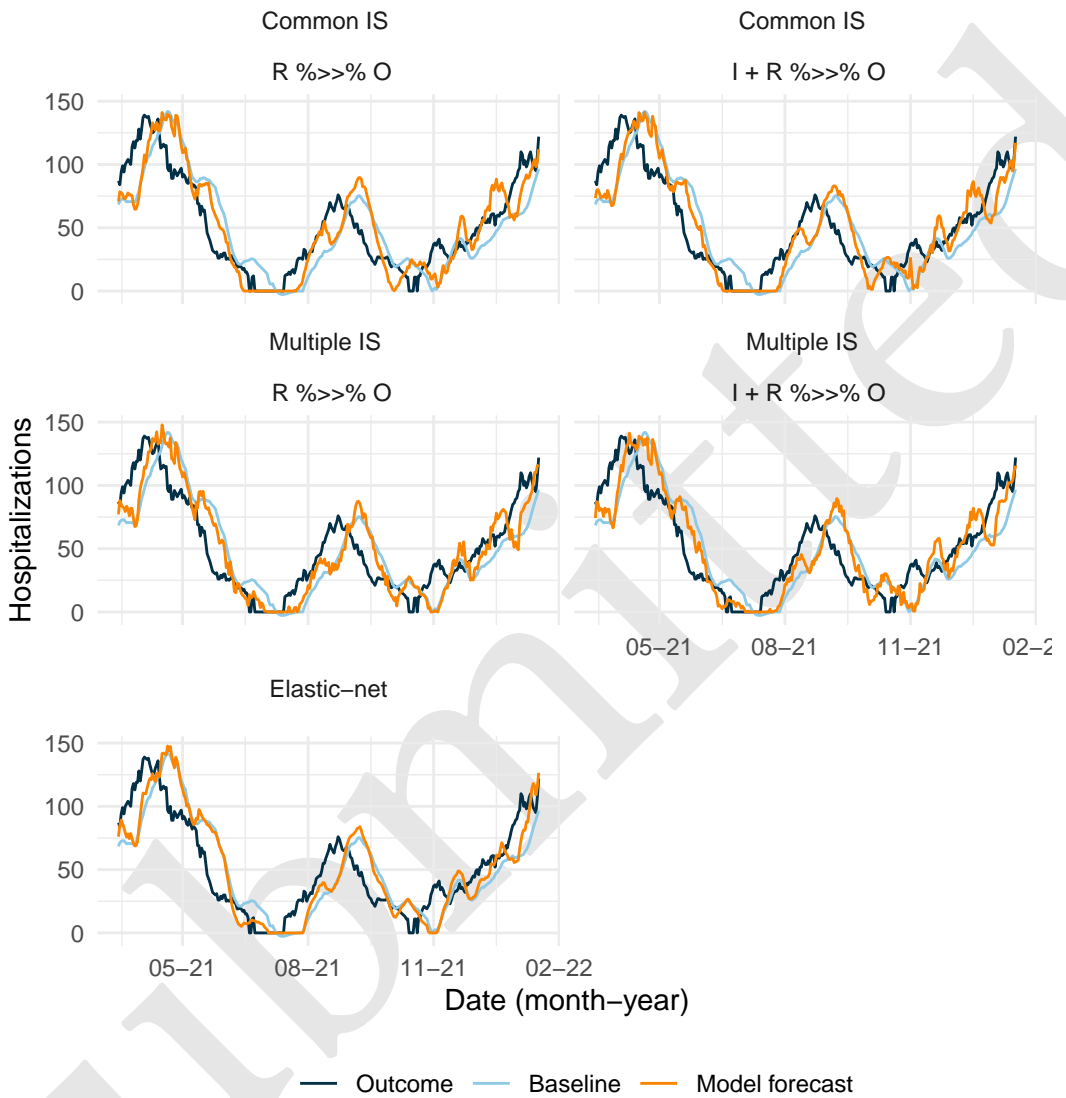


Figure 14: Reservoir computing forecast depending on the setting with and without monthly update. Red line is the median forecast of 40 reservoirs. Grey lines are individual forecast of each of the 40 reservoirs.

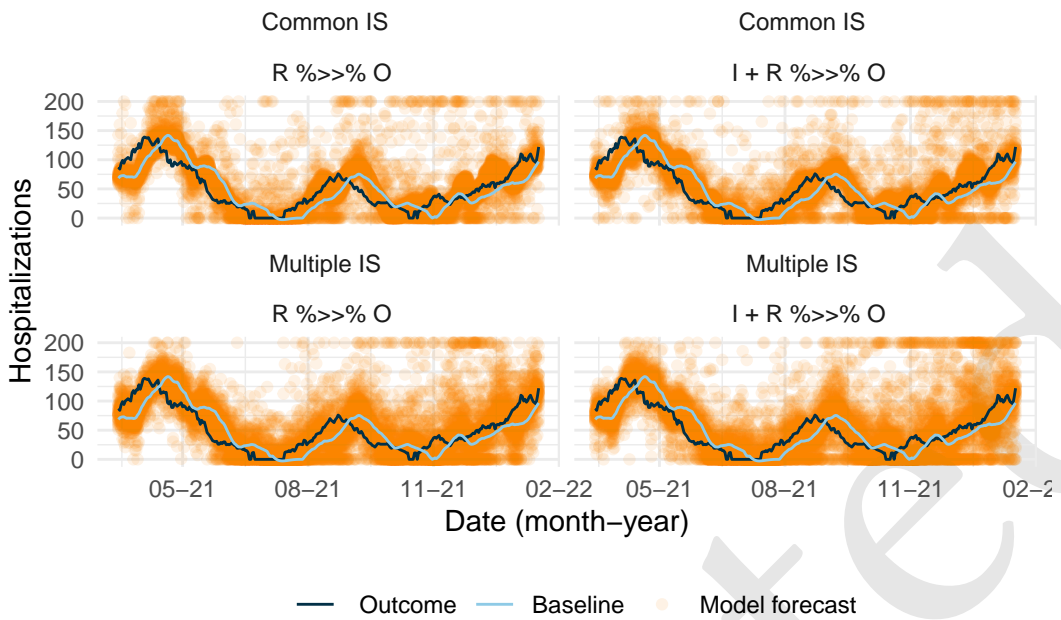


Figure 15: Individual forecast the 40 best hyperparameter sets for the different RC configuration. Forecast value above 200 were set to 200 for clarity.

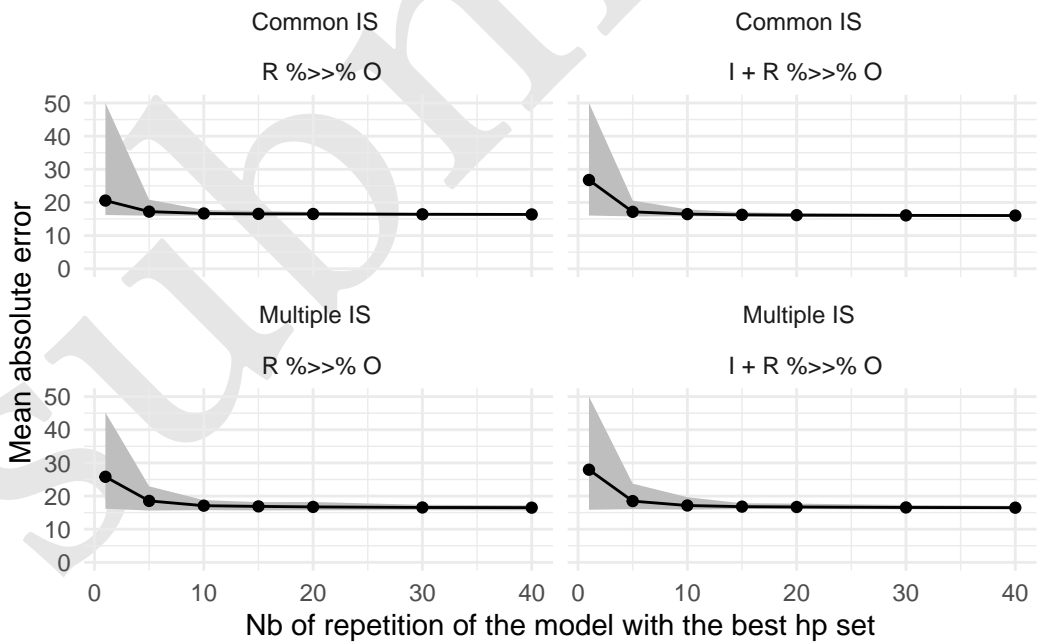


Figure 16: Mean absolute error depending on the number of aggregated reservoir.

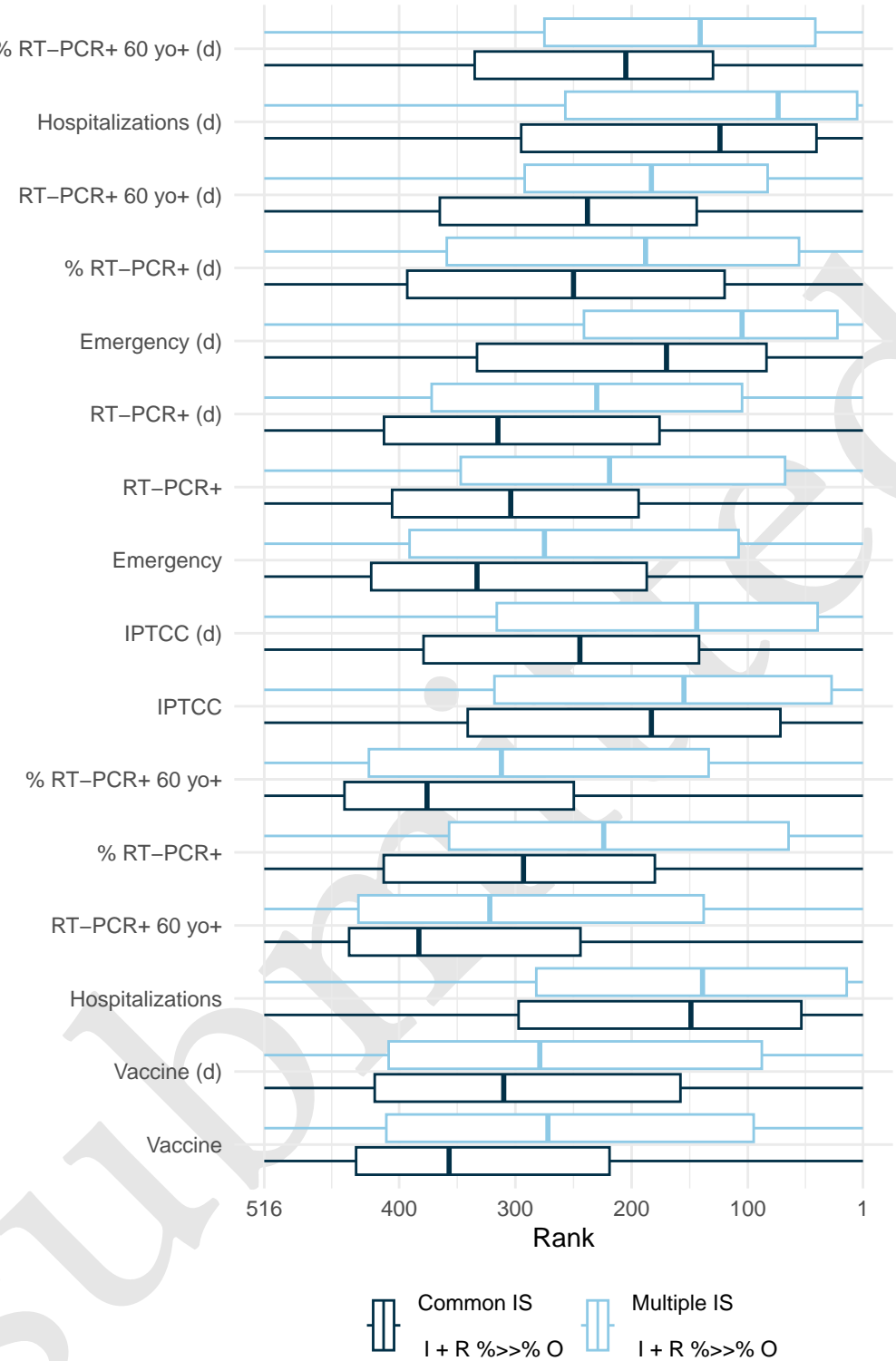


Figure 17: Mean feature importance of the 40 best hyperparameter sets by model, focus on the connection between the input and output layers. Models with direct connection between input and output layer are included. The rank is obtained by comparing the feature input layer and all other connection coefficients (both input and reservoir corresponding coefficients) attributed by the output layer at each date for each hyperparameter set. The higher the output layer's coefficient for the input layer, the closer its rank will be to 1 and the more important the feature is.

Furthermore, Figure 18 compares the coefficients assigned to input features by the elastic-net model and the RC models. While the coefficients are generally consistent across RC models, there are some notable differences with elastic-net. Specifically, certain features deemed important by the elastic-net model, such as the derivative of RT-PCR, and the derivative of Vaccine, are less important for the reservoir computing model. This may indicate that these features predictive ability is better conveyed by their relationship with other features, which is captured by the reservoir computing model but might not be by the elastic-net model. Conversely, emergency, IPTCC, proportion of positive RT-PCR, and hospitalizations are more important for the reservoir computing model than for the elastic-net model.

4.4 Discussion

In this specific application, we have demonstrated that RC exhibits commendable performance in comparison to Elastic-net, which serves as the reference model. Furthermore, we highlight the inherent challenges in forecasting within this context, primarily stemming from the non-stationarity of the time series.

All computations in this study were conducted using the `reservoirnet` package, and the entire codebase is accessible on Zenodo (Ferté et al. 2024). This R package demonstrates its efficacy in implementing various reservoir architectures, including connection between the input layer and the output layer, as well as the utilization of several input scaling, all within the context of a real-world use case.

Given the substantial number of hyperparameters involved, we acknowledge that random search may not be the most efficient optimization algorithm. We have retained this approach for the sake of simplicity in this tutorial paper; however, meta-heuristic approaches, particularly those utilizing evolutionary algorithms, may prove more efficient, especially when employing multiple input scaling (Bala et al. 2018).

This study represents a novel contribution to epidemic forecasting utilizing RC. Notably, previous literature predominantly focused on simpler problems characterized by fewer input features or shorter evaluation periods Ghosh et al. (2021). Our findings underscore the potential of this approach for future epidemics, suggesting its potential to surpass more traditional epidemiological tools while maintaining a lightweight model structure compared to other RNNs.

It is worth noting that all models, including the Ferté et al. (2022) models, encounter challenges in accurately anticipating slope shifts, indicating the need for further investigation. Specifically, additional work is warranted to extend the application of RC to high-dimensional settings, building upon the insights gained from models based on a more extensive set of features.

5 Discussion and conclusion

In this paper, we introduce the R package `reservoirnet`, which serves as a versatile tool for implementing reservoir computing based on `ReservoirPy`'s Python library. It offers flexibility in defining the reservoir architecture, including options for specifying connections between the input layer and the output layer, as well as variations in input scaling as demonstrated on a real-world use case.

We provided a comprehensive overview of the basic usage of the `reservoirnet` package through illustrative examples in regression and classification tasks. This introductory section serves as a foundation for R users, offering step-by-step guidance on constructing and training reservoir computing models using the package. By demonstrating the application of RC in both regression and

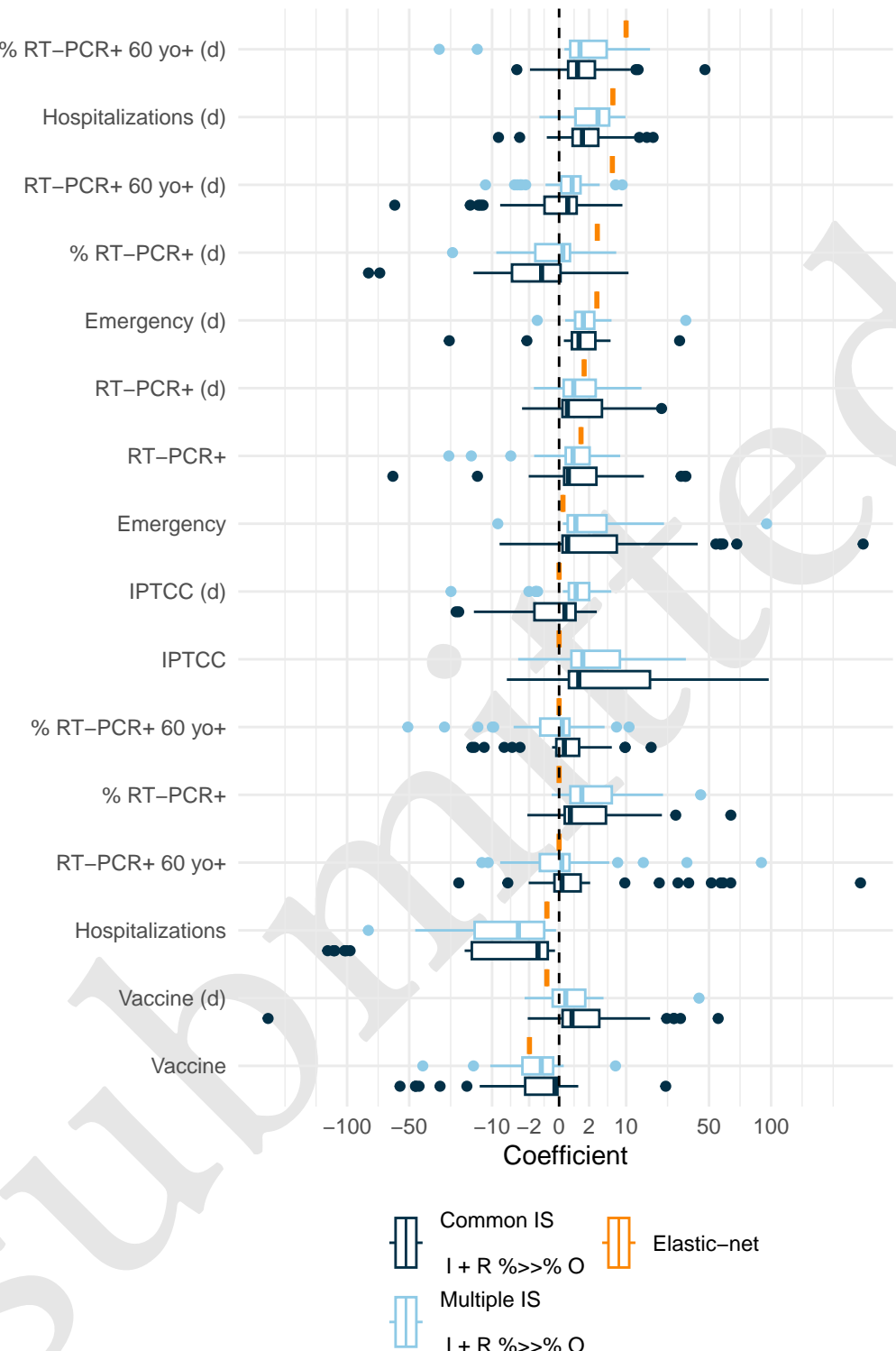


Figure 18: Mean feature coefficient of the 40 best hyperparameter sets by model and the elastic-net model. Only models with direct connection between input and output layer are included. The coefficients were calculated as the average value across all dates for each feature, model and hyperparameter set.

480 classification scenarios, we aim to equip users with the essential knowledge and skills needed to
481 harness the capabilities of reservoir computing for diverse tasks.

482 Drawing on the robust foundation of the ReservoirPy structure, a well-maintained Python library,
483 this package inherits its reliability and longevity. We have focused on providing access to the fun-
484 damental features, building upon the strong base provided by ReservoirPy. Therefore, this initial
485 version of reservoirnet must evolve in tandem with the growing understanding and adoption of
486 RC within the R community.

487 References

- 488 Bala, Abubakar, Idris Ismail, Rosdiazli Ibrahim, and Sadiq M. Sait. 2018. “Applications of Meta-
489 heuristics in Reservoir Computing Techniques: A Review.” *IEEE Access* 6: 58012–29. <https://doi.org/10.1109/ACCESS.2018.2873770>.
- 490 Carrat, Fabrice, Julie Figoni, Joseph Henny, Jean-Claude Desenclos, Sofiane Kab, Xavier de Lambal-
491 lerie, and Marie Zins. 2021. “Evidence of Early Circulation of SARS-CoV-2 in France: Findings
492 from the Population-Based ‘CONSTANCES’ Cohort.” *European Journal of Epidemiology*, Febru-
493 ary, 1–4. <https://doi.org/10.1007/s10654-020-00716-2>.
- 494 Carslaw, David. 2023. “Worldmet: Import Surface Meteorological Data from NOAA Integrated
495 Surface Database (ISD).” <https://cran.r-project.org/web/packages/worldmet/index.html>.
- 496 Carvalho, Kathleen, João Paulo Vicente, Mihajlo Jakovljevic, and João Paulo Ramos Teixeira. 2021.
497 “Analysis and Forecasting Incidence, Intensive Care Unit Admissions, and Projected Mortality
498 Attributable to COVID-19 in Portugal, the UK, Germany, Italy, and France: Predictions for 4
499 Weeks Ahead.” *Bioengineering* 8 (6): 84. <https://doi.org/10.3390/bioengineering8060084>.
- 500 COVID-19 Cumulative Infection Collaborators. 2022. “Estimating Global, Regional, and National
501 Daily and Cumulative Infections with SARS-CoV-2 Through Nov 14, 2021: A Statistical Analy-
502 sis.” *Lancet*. [https://doi.org/10.1016/S0140-6736\(22\)00484-6](https://doi.org/10.1016/S0140-6736(22)00484-6).
- 503 Cramer, Estee Y., Evan L. Ray, Velma K. Lopez, Johannes Bracher, Andrea Brennen, and et al. 2022.
504 “Evaluation of Individual and Ensemble Probabilistic Forecasts of COVID-19 Mortality in the
505 United States.” *Proceedings of the National Academy of Sciences* 119 (15): e2113561119. <https://doi.org/10.1073/pnas.2113561119>.
- 506 Etalab. 2020. “Les Données Relatives Au COVID-19 En France - Data.gouv.fr.” <https://www.data.gouv.fr/fr/pages/donnees-coronavirus/>.
- 507 Ferté, Thomas, Kalidou Ba, Dan Dutartre, Pierrick Legrand, Vianney Jouhet, Romain Griffier,
508 Rodolphe Thiébaut, Xavier Hinaut, and Boris P. Hejblum. 2024. “Thomasferte/Jss_reservoirnet:
509 First Release.” Zenodo. <https://doi.org/10.5281/ZENODO.11281341>.
- 510 Ferté, Thomas, Vianney Jouhet, Romain Griffier, Boris P. Hejblum, Rodolphe Thiébaut, and Bordeaux
511 University Hospital Covid-19 Crisis Task Force. 2022. “The Benefit of Augmenting Open Data
512 with Clinical Data-Warehouse EHR for Forecasting SARS-CoV-2 Hospitalizations in Bordeaux
513 Area, France.” *JAMIA Open* 5 (4): ooac086. <https://doi.org/10.1093/jamiaopen/ooac086>.
- 514 Ferté, Thomas, Vianney Jouhet, Romain Griffier, Boris Hejblum, Rodolphe Thiébaut, and Bordeaux
515 University Hospital Covid-19 Crisis Task Force. 2023. “The Benefit of Augmenting Open Data
516 with Clinical Data-Warehouse EHR for Forecasting SARS-CoV-2 Hospitalizations in Bordeaux
517 Area, France.” Dryad. <https://doi.org/10.5061/DRYAD.HHMGQNKX>.
- 518 Friedman, Jerome, Trevor Hastie, and Rob Tibshirani. 2010. “Regularization Paths for Generalized
519 Linear Models via Coordinate Descent.” *Journal of Statistical Software* 33 (1): 1–22.
- 520 Ghosh, Subrata, Abhishek Senapati, Arindam Mishra, Joydev Chattopadhyay, Syamal K. Dana, Chit-
521 taranjan Hens, and Dibakar Ghosh. 2021. “Reservoir Computing on Epidemic Spreading: A Case
522 Study on COVID-19 Cases.” *Physical Review E* 104 (1): 014308. <https://doi.org/10.1103/PhysRevE.104.014308>.

- 527 Hinaut, Xavier, and Peter Ford Dominey. 2013. “Real-Time Parallel Processing of Grammatical
528 Structure in the Fronto-Striatal System: A Recurrent Network Simulation Study Using Reser-
529 voir Computing.” *PLOS ONE* 8 (2): e52946. <https://doi.org/10.1371/journal.pone.0052946>.
- 530 Hübner, Martin, Tobias Zingg, David Martin, Philippe Eckert, and Nicolas Demartines. 2020.
531 “Surgery for Non-Covid-19 Patients During the Pandemic.” *PLoS ONE* 15 (10): e0241331.
532 <https://doi.org/10.1371/journal.pone.0241331>.
- 533 Jaeger, Herbert. 2001. “The” Echo State” Approach to Analysing and Training Recurrent Neural
534 Networks-with an Erratum Note.” *Bonn, Germany: German National Research Center for Infor-
535 mation Technology GMD Technical Report* 148 (January).
- 536 Kim, Gina, Mengru Wang, Hanh Pan, Giana H. Davidson, Alison C. Roxby, Jen Neukirch, Danna Lei,
537 Elicia Hawken-Dennis, Louise Simpson, and Thuan D. Ong. 2020. “A Health System Response
538 to COVID-19 in Long-Term Care and Post-Acute Care: A Three-Phase Approach.” *Journal of the
539 American Geriatrics Society* 68 (6): 1155–61. <https://doi.org/10.1111/jgs.16513>.
- 540 Kmet, Tibor, and Maria Kmetova. 2019. “Bézier Curve Parametrisation and Echo State Network
541 Methods for Solving Optimal Control Problems of SIR Model.” *Biosystems* 186 (December):
542 104029. <https://doi.org/10.1016/j.biosystems.2019.104029>.
- 543 Kudo, Mineichi, Jun Toyama, and Masaru Shimbo. 1999. “Multidimensional Curve Classification
544 Using Passing-Through Regions.” *Pattern Recognition Letters* 20 (11): 1103–11. [https://doi.org/10.1016/S0167-8655\(99\)00077-X](https://doi.org/10.1016/S0167-8655(99)00077-X).
- 545 Liu, Bocheng, Yiyuan Xie, Weichen Liu, Xiao Jiang, Yichen Ye, Tingting Song, Junxiong Chai, Many-
546 ing Feng, and Haodong Yuan. 2023. “Nanophotonic Reservoir Computing for COVID-19 Pan-
547 demic Forecasting.” *Nonlinear Dynamics* 111 (7): 6895–6914. [https://doi.org/10.1007/s11071-022-08190-z](https://doi.org/10.1007/s11071-022-
548 08190-z).
- 549 Lukoševičius, Mantas, and Herbert Jaeger. 2009. “Reservoir Computing Approaches to Recurrent
550 Neural Network Training.” *Computer Science Review* 3 (3): 127–49. [https://doi.org/10.1016/j.cosrev.2009.03.005](https://doi.org/10.1016/j.
551 cosrev.2009.03.005).
- 552 Maass, Wolfgang, Thomas Natschläger, and Henry Markram. 2002. “Real-Time Computing With-
553 out Stable States: A New Framework for Neural Computation Based on Perturbations.” *Neural
554 Computation* 14 (11): 2531–60. <https://doi.org/10.1162/089976602760407955>.
- 555 Martinuzzi, Francesco, Chris Rackauckas, Anas Abdelrehim, Miguel D. Mahecha, and Karin Mora.
556 2022. “ReservoirComputing.jl: An Efficient and Modular Library for Reservoir Computing Mod-
557 els.” *Journal of Machine Learning Research* 23 (288): 1–8. <http://jmlr.org/papers/v23/22-0611.html>.
- 558 Mohimont, Lucas, Amine Chemchem, François Alin, Michaël Krajecki, and Luiz Angelo Steffenel.
559 2021. “Convolutional Neural Networks and Temporal CNNs for COVID-19 Forecasting in
560 France.” *Applied Intelligence*, April. <https://doi.org/10.1007/s10489-021-02359-6>.
- 561 Nakane, Ryosho, Gouhei Tanaka, and Akira Hirose. 2018. “Reservoir Computing With Spin Waves
562 Excited in a Garnet Film.” *IEEE Access PP* (January): 1–1. [https://doi.org/10.1109/ACCESS.2018.2794584](https://doi.org/10.1109/ACCESS.2018.
563 2794584).
- 564 Paireau, Juliette, Alessio Andronico, Nathanaël Hozé, Maylis Layen, Pascal Crépey, Alix Roumagnac,
565 Marc Lavielle, Pierre-Yves Boëlle, and Simon Cauchemez. 2022. “An Ensemble Model Based
566 on Early Predictors to Forecast COVID-19 Health Care Demand in France.” *Proceedings of the
567 National Academy of Sciences* 119 (18): e2103302119. <https://doi.org/10.1073/pnas.2103302119>.
- 568 Penkovsky, Bogdan, Laurent Larger, and Daniel Brunner. 2018. “Efficient Design of Hardware-
569 Enabled Reservoir Computing in FPGAs.” *Journal of Applied Physics* 124 (16): 162101. [https://doi.org/10.1063/1.5039826](https://
570 doi.org/10.1063/1.5039826).
- 571 Pottier, Loïc. 2021. “Forecast of the Covid19 Epidemic in France.” *medRxiv*. [https://doi.org/10.1101/2021.04.13.21255418](https://doi.org/10.1101/
572 2021.04.13.21255418).
- 573 Prychynenko, Diana, Matthias Sitte, Kai Litzius, Benjamin Krüger, George Bourianoff, Mathias
574 Kläui, Jairo Sinova, and Karin Everschor-Sitte. 2018. “Magnetic Skyrmion as a Nonlinear Re-

- 577 sistive Element: A Potential Building Block for Reservoir Computing.” *Physical Review Applied*
578 9 (1): 014034. <https://doi.org/10.1103/PhysRevApplied.9.014034>.
- 579 Rafayelyan, Mushegh, Jonathan Dong, Yongqi Tan, Florent Krzakala, and Sylvain Gigan. 2020.
580 “Large-Scale Optical Reservoir Computing for Spatiotemporal Chaotic Systems Prediction.”
581 *Physical Review X* 10 (4): 041037. <https://doi.org/10.1103/PhysRevX.10.041037>.
- 582 Rahimi, Iman, Fang Chen, and Amir H. Gandomi. 2021. “A Review on COVID-19 Forecasting
583 Models.” *Neural Computing & Applications*, February, 1–11. <https://doi.org/10.1007/s00521-020-05626-8>.
- 585 Ray, Arnob, Tanujit Chakraborty, and Dibakar Ghosh. 2021. “Optimized Ensemble Deep Learning
586 Framework for Scalable Forecasting of Dynamics Containing Extreme Events.” *Chaos (Wood-
587 bury, N.Y.)* 31 (11): 111105. <https://doi.org/10.1063/5.0074213>.
- 588 Roumagnac, Alix, Eurico de Carvalho Filho, Raphaël Bertrand, Anne-Kim Banchereau, and Guil-
589 laume Lahache. 2021. “Étude de l’influence Potentielle de l’humidité Et de La Température
590 Dans La Propagation de La Pandémie COVID-19.” *Médecine de Catastrophe - Urgences Collec-
591 tives, Douleur et situations d’exceptionPandémie COVID-19*, 5 (1): 87–102. <https://doi.org/10.1016/j.pxur.2021.01.002>.
- 593 Simões, Jorge, João Paulo Moreira Magalhães, André Biscaia, António da Luz Pereira, Gonçalo
594 Figueiredo Augusto, and Inês Fronteira. 2021. “Organisation of the State, Model of Health Sys-
595 tem and COVID-19 Health Outcomes in Six European Countries, During the First Months of
596 the COVID-19 Epidemic in 2020.” *The International Journal of Health Planning and Management*,
597 June, 10.1002/hpm.3271. <https://doi.org/10.1002/hpm.3271>.
- 598 Smith, Adam, Neal Lott, and Russ Vose. 2011. “The Integrated Surface Database: Recent De-
599 velopments and Partnerships.” *Bulletin of the American Meteorological Society* 92 (6): 704–8.
600 <https://doi.org/10.1175/2011BAMS3015.1>.
- 601 Tanaka, Gouhei, Toshiyuki Yamane, Jean Benoit Héroux, Ryosho Nakane, Naoki Kanazawa, Seiji
602 Takeda, Hidetoshi Numata, Daiju Nakano, and Akira Hirose. 2019. “Recent Advances in Physical
603 Reservoir Computing: A Review.” *Neural Networks* 115 (July): 100–123. <https://doi.org/10.1016/j.neunet.2019.03.005>.
- 605 Trouvain, Nathan, and Xavier Hinaut. 2021. “Canary Song Decoder: Transduction and Implicit
606 Segmentation with ESNs and LTSMs.” In *Artificial Neural Networks and Machine Learning –
607 ICANN 2021*, edited by Igor Farkaš, Paolo Masulli, Sebastian Otte, and Stefan Wermter, 71–82.
608 Lecture Notes in Computer Science. Cham: Springer International Publishing. https://doi.org/10.1007/978-3-030-86383-8_6.
- 610 ———. 2022. “Reservoirpy: A Simple and Flexible Reservoir Computing Tool in Python.” <https://inria.hal.science/hal-03699931>.
- 612 Trouvain, Nathan, Luca Pedrelli, Thanh Trung Dinh, and Xavier Hinaut. 2020. “ReservoirPy: An
613 Efficient and User-Friendly Library to Design Echo State Networks.” In *Artificial Neural Networks
614 and Machine Learning – ICANN 2020*, 494–505. Springer International Publishing. <https://inria.hal.science/hal-02595026>.
- 616 Trouvain, Nathan, Nicolas Rougier, and Xavier Hinaut. 2022. “Create Efficient and Complex Reser-
617 voir Computing Architectures with ReservoirPy.” In *From Animals to Animats 16*, edited by Lola
618 Cañamero, Philippe Gaussier, Myra Wilson, Sofiane Boucenna, and Nicolas Cuperlier, 91–102.
619 Lecture Notes in Computer Science. Cham: Springer International Publishing. https://doi.org/10.1007/978-3-031-16770-6_8.
- 621 Ushey, Kevin, JJ Allaire, and Yuan Tang. 2024. *Reticulate: Interface to ‘Python’*. <https://rstudio.github.io/reticulate/>.
- 623 Vlachas, P. R., J. Pathak, B. R. Hunt, T. P. Sapsis, M. Girvan, E. Ott, and P. Koumoutsakos. 2020.
624 “Backpropagation Algorithms and Reservoir Computing in Recurrent Neural Networks for the
625 Forecasting of Complex Spatiotemporal Dynamics.” *Neural Networks* 126 (June): 191–217. <https://doi.org/10.1016/j.neunet.2020.02.016>.

- 627 Wickham, Hadley, Romain François, Lionel Henry, Kirill Müller, and Davis Vaughan. 2023. “dplyr:
628 A Grammar of Data Manipulation.” <https://CRAN.R-project.org/package=dplyr>.
- 629 Wickham, Hadley, Danielle Navarro, and Thomas Lin Pedersen. 2018. *ggplot2: Elegant Graphics for*
630 *Data Analysis (3e)*. 3rd ed. Springer-Verlag New York. <https://ggplot2-book.org/>.
- 631 World Health Organisation. 2020. “WHO Coronavirus (COVID-19) Dashboard.” [https://covid19.](https://covid19.who.int)
632 [who.int](https://covid19.who.int).
- 633 Zhang, Qihuang, Grace Y. Yi, Li-Pang Chen, and Wenqing He. 2023. “Sentiment Analysis and Causal
634 Learning of COVID-19 Tweets Prior to the Rollout of Vaccines.” *PloS One* 18 (2): e0277878.
635 <https://doi.org/10.1371/journal.pone.0277878>.

Submitted